American Mineralogist, Volume 74, pages 593–598, 1989

Crystal-chemical study of cation disordering in Al-rich and Al-poor orthopyroxenes from spinel lherzolite xenoliths

G. M. MOLIN

Dipartimento di Mineralogia e Petrologia, Corso Garibaldi 37, Università di Padova, 35100 Padova, Italy

ABSTRACT

Structural refinements of natural and heated orthopyroxenes from two spinel lherzolite xenoliths were used to investigate the extent of disordering of Mg and Fe^{2+}, and of the trivalent cations, in the orthopyroxene crystal structures.

The orthopyroxenes were studied both before and after heating. Although disordering of Mg and Fe^{2+} between M1 and M2 sites was increased at high temperatures (1050–1150 °C), trivalent cations continued to be restricted to M1 sites. Disordering of Mg and Fe^{2+} was more easily achieved when contents of trivalent cations in the orthopyroxene are low.

INTRODUCTION

Ultramafic xenoliths from basaltic rocks and kimberlites are of interest because they are generally thought to be samples of the upper mantle and because they may provide clues to processes of basaltic magma generation. Molin and Varne (in prep.) have made a crystal-chemical study of the orthopyroxenes from a suite of spinel lherzolite xenoliths from Mount Leura and Mount Porndon, two of the centers of basanitic volcanism of the Newer Volcanics of western Victoria, Australia, and have found that their orthopyroxenes are R_2O_3-bearing enstatites, similar in composition to orthopyroxenes of spinel lherzolite xenoliths worldwide.

The crystal-chemical characteristics of the orthopyroxenes from these xenoliths are mainly due to the substitution

$$(\mathrm{Fe}^{2+}_{(\mathrm{M1+M2})}{}^{[6]}\mathrm{Al}),{}^{[4]}\mathrm{Al} \leftrightarrow (\mathrm{MgCr}^{3+}),\mathrm{Si}.$$

The principal cation substitution ($^{[6]}$Al-Mg) involves the M1 site and is responsible for the small cell volumes that characterize these orthopyroxenes, which probably reflect their crystallization at high pressures. With increasing Mg content in M1 and M2, Fe^{2+} depletion was found to occur in both sites. However, when relatively Mg-poor orthopyroxenes $[Mg/(Mg + Fe^{2+}) = 0.908]$ are compared with relatively Mg-rich orthopyroxenes $[Mg/(Mg + Fe^{2+}) = 0.93]$, Molin and Varne (in prep.) found that whereas Fe^{2+} in M1 tends toward zero, a considerable amount of Fe^{2+} (about 0.12 Fe^{2+} per formula unit, pfu) is retained in M2, showing that Mg-Fe^{2+} are fairly well ordered. In addition, the trivalent cations (Al, Cr, Fe^{3+}) seem to be restricted to the M1 site.

It is well known that Mg-Fe^{2+} disorder in orthopyroxenes is temperature-dependent, but the extent of disordering in Mg-rich compositions at high temperatures has not yet been investigated. Moreover, Ganguly and Ghose (1979) have suggested that "octahedral Al disorders between M1 and M2 sites with preference for M1," and have developed a thermodynamic model to explain this postulated $^{[6]}$Al disordering as a function of temperature and composition. Although Domeneghetti et al. (1985) and Tazzoli and Domeneghetti (1987) failed to observe $^{[6]}$Al disordering in more Fe-rich orthopyroxenes, its possible extent in Mg-rich compositions again remains uninvestigated.

It is therefore of interest to evaluate the possible effects of high temperatures on the distribution of $^{[6]}$Al between the M1 and M2 sites in orthopyroxenes from spinel lherzolite xenoliths, and to assess the extent to which Mg-Fe^{2+} ions become disordered in Mg-rich orthopyroxene with increasing temperature, particularly because most methods of estimating the temperatures of crystallization of spinel lherzolite assemblages rely on a solution-model approach to pyroxene thermometry.

EXPERIMENTAL TECHNIQUES

Two orthopyroxene crystals (Table 1: Le4A, Le9A) were selected for experimental study from two members of a suite of spinel lherzolite xenoliths from Mount Leura, a center of basanitic volcanism in western Victoria, Australia. Dal Negro et al. (1984) have already thoroughly studied the composition and crystal-chemistry of clinopyroxenes from this xenolith suite; Della Giusta et al. (1986) have studied some of the spinels, Princivalle and Secco (1985), some olivines, and Molin and Varne (in prep.), the orthopyroxenes.

The two orthopyroxenes were chosen because they have similar $[Mg/(Mg + Fe^{2+})]$ values (0.922 for Le4A; 0.921 for Le9A), but different contents of Al_2O_3 (3.9 wt% for Le4A; 0.4 wt% for Le9A). Le4A shows a higher degree of ordering of Mg-Fe^{2+} than Le9A, as expressed by the values of K_D ($K_D = \mathrm{Fe}^{2+}_{\mathrm{M1}}\mathrm{Mg}^{2+}_{\mathrm{M2}}/\mathrm{Fe}^{2+}_{\mathrm{M2}}\mathrm{Mg}^{2+}_{\mathrm{M1}}$) (Table 1), because of the absence of Fe^{2+} from its M1 site.

Following petrographic examination and microprobe analysis of the minerals of the xenoliths, representative orthopyroxenes were extracted from polished sections about 100 μm in thickness.

0003–004X/89/0506–0593$02.00

TABLE 1. Chemical composition and site occupancy of orthopyroxenes

	Le4A	Le9A		Le4A	Le9A
			M1 site		
SiO_2	55.0	57.5	Mg	0.896	0.965
TiO_2	0.12	0.10	Fe^{2+}	0.000	0.017
Al_2O_3	3.9	0.4	Fe^{3+}	0.039	0.004
FeO	6.3	6.0	Cr	0.007	0.014
MnO	0.24	0.00	Ti^{4+}	0.003	0.000
MgO	33.4	35.2	$^{[6]}Al$	0.055	0.000
CaO	0.78	0.30		1.000	1.000
Cr_2O_3	0.26	0.44	**M2 site**		
	100.00	99.84	Mg	0.818	0.847
Si sites			Fe^{2+}	0.145	0.139
Si	1.895	1.984	Ca	0.029	0.014
$^{[4]}Al$	0.105	0.016	Mn	0.008	0.000
	2.000	2.000		1.000	1.000
			$Mg/(Mg + Fe^{2+})$	0.922	0.921
			K_D*	0.00	0.11

* $K_D = Fe^{2+}_{M1}Mg_{M2}/Fe^{2+}_{M2}Mg_{M1}$.

Microprobe analysis

First, the chemical compositions of the selected orthopyroxene crystals were obtained by electron-microprobe analysis. Each crystal fragment was analyzed in about six spots on each of its surfaces, and the resulting data were averaged to obtain the compositions given in Table 1. The analytical system used an EDS EG&G energy-dispersive spectrometer on an Autoscan SEM electron microscope operating at 15 kV. X-ray counts were converted

TABLE 2. Structural data of natural and heated orthopyroxenes

	Le4A					
	Natural	1050 °C 3 min	1050 °C 10 min	1050 °C 90 min	1150 °C 2 min	1150 °C 10 min
a (Å)	18.241(2)	18.244(2)	18.243(2)	18.244(1)	18.246(2)	18.242(2)
b (Å)	8.804(1)	8.805(1)	8.808(1)	8.805(1)	8.809(1)	8.803(1)
c (Å)	5.198(1)	5.196(1)	5.197(1)	5.196(1)	5.197(1)	5.198(1)
V (Å³)	834.77	834.77	835.06	834.64	835.32	834.76
*N**	1039	1045	1043	1042	1050	1045
R (%)**	2.0	2.2	2.2	2.5	2.2	2.6
M1–O1A	2.023(1)	2.024(2)	2.025(1)	2.023(2)	2.025(1)	2.023(2)
M1–O1A	2.142(1)	2.143(2)	2.143(1)	2.147(2)	2.145(1)	2.143(2)
M1–O1B	2.052(1)	2.052(2)	2.053(1)	2.053(2)	2.054(1)	2.055(2)
M1–O1B	2.155(1)	2.156(2)	2.157(1)	2.155(2)	2.159(1)	2.156(2)
M1–O2A	2.005(1)	2.008(2)	2.005(1)	2.005(2)	2.008(1)	2.007(2)
M1–O2B	2.031(1)	2.031(2)	2.032(1)	2.032(2)	2.032(2)	2.032(2)
Mean	2.068	2.069	2.069	2.069	2.071	2.069
V (Å³)	11.66	11.67	11.67	11.68	11.70	11.68
M2–O1A	2.132(1)	2.131(2)	2.131(1)	2.131(2)	2.131(1)	2.133(2)
M2–O1B	2.081(1)	2.078(2)	2.079(1)	2.078(2)	2.077(1)	2.077(2)
M2–O2A	2.061(1)	2.061(2)	2.064(1)	2.060(2)	2.061(1)	2.061(2)
M2–O2B	1.999(1)	1.998(2)	2.002(1)	1.996(2)	1.999(2)	1.996(2)
M2–O3A	2.303(1)	2.303(2)	2.302(1)	2.302(2)	2.303(1)	2.301(2)
M2–O3B	2.399(1)	2.399(2)	2.398(1)	2.401(2)	2.397(1)	2.401(2)
Mean	2.163	2.161	2.162	2.161	2.161	2.161
V (Å³)	12.58	12.56	12.59	12.56	12.57	12.56
SiA–O1A	1.615(1)	1.615(1)	1.615(1)	1.613(2)	1.614(1)	1.614(2)
SiA–O2A	1.594(1)	1.593(2)	1.593(1)	1.594(2)	1.591(1)	1.592(2)
SiA–O3A	1.645(1)	1.645(2)	1.646(1)	1.646(2)	1.644(1)	1.646(2)
SiA–O3A	1.661(1)	1.661(2)	1.662(1)	1.661(2)	1.663(1)	1.662(2)
Mean	1.629	1.628	1.629	1.628	1.628	1.628
V (Å³)	2.188	2.187	2.190	2.187	2.186	2.187
SiB–O1B	1.632(1)	1.633(1)	1.633(1)	1.633(2)	1.633(1)	1.632(2)
SiB–O2B	1.601(1)	1.601(2)	1.600(1)	1.600(2)	1.601(1)	1.601(2)
SiB–O3B	1.677(1)	1.676(2)	1.680(1)	1.674(2)	1.679(2)	1.674(2)
SiB–O3B	1.684(1)	1.684(2)	1.681(1)	1.685(2)	1.684(1)	1.685(2)
Mean	1.648	1.648	1.649	1.647	1.649	1.648
V (Å³)	2.283	2.283	2.284	2.279	2.287	2.281

* Number of observed reflections.

** Observed *R* discrepancy factor × 100.

into oxide weight percentages using a MAGIC program (Colby, 1972) in the ORTEC MAGIC IV version, and the results were compared against a Kakanui augite standard. Typically, the analyses of SiO_2, Al_2O_3, FeO, MgO, and CaO, which make up about 99 wt% of the orthopyroxene analyses of Table 1, are accurate to within 2% of the amount present. The accuracy of the analyses is also checked against the X-ray diffraction measurements of the M1 and M2 site electron densities, which provide an independent evaluation of the chemical composition (see cation distribution).

Single-crystal X-ray diffractometry

Single-crystal X-ray diffraction data were then obtained for the analyzed crystal fragments of Le4A and Le9A orthopyroxenes by using a computer-controlled SIEMENS AED four-circle diffractometer with Mo*Kα* radiation monochromatized by a flat graphite crystal. The equivalent pairs *hkl* and $-hkl$ were measured up to $\theta \leq 30°$ using the ω-scan mode. Intensities were corrected for absorption following the semi-empirical method of North et al. (1968), and the values of equivalent pairs were averaged. The refinements were carried out in space group *Pbca* without chemical constraints using the STRUCSY program distributed by STOE. The adopted ionization scheme (Rossi et al., 1983) was 2.5 positive charges for Si, 1.5 negative charges for oxygen, and 2 positive charges for Mg and Fe. The atomic scattering factors were taken from *International Tables for X-ray Crystallography* (1974) and Tokonami (1965). All the structural sites were considered fully occupied. In the first stages of the refinements, isotropic temperature factors were used. The final cycles were performed allowing all parameters [atomic coordinates, anisotropic temperature factors, M1 and M2 site occupancies, scale factors and secondary extinction coefficients (Zachariasen, 1963)] to vary until the shifts were less than the least-squares difference of the corresponding parameters. The reflections with $I > 3\sigma(I)$ were considered as observed and were given equal weighting when used in the refinement procedure. Structural data and estimated standard deviations are reported in Table 2.

Cation distribution

Cation distributions among sites (Table 1) were obtained by the minimization of the squares of the following constraints: (1) balance between atomic fractions and site

TABLE 2.—*Continued*

Le9A					
Natural	1050 °C 3 min	1050 °C 10 min	1050 °C 90 min	1150 °C 2 min	1150 °C 10 min
18.246(2)	18.250(2)	18.250(2)	18.248(1)	18.248(2)	18.243(2)
8.828(1)	8.830(1)	8.829(1)	8.831(1)	8.832(1)	8.834(1)
5.189(1)	5.190(1)	5.191(1)	5.189(1)	5.192(1)	5.190(1)
835.89	836.40	836.38	836.27	836.77	836.32
1041	1045	1021	1029	1042	1053
1.9	2.0	1.9	2.0	2.1	2.0
2.027(1)	2.027(1)	2.029(1)	2.028(1)	2.031(1)	2.029(1)
2.150(1)	2.149(1)	2.151(1)	2.151(1)	2.149(1)	2.150(1)
2.062(1)	2.066(1)	2.065(1)	2.064(1)	2.062(1)	2.063(1)
2.166(1)	2.166(1)	2.167(1)	2.167(1)	2.170(1)	2.170(1)
2.012(1)	2.012(1)	2.014(1)	2.012(1)	2.013(1)	2.013(1)
2.048(1)	2.046(1)	2.047(1)	2.046(1)	2.048(1)	2.048(1)
2.078	2.078	2.079	2.078	2.079	2.079
11.82	11.82	11.84	11.83	11.84	11.84
2.113(1)	2.114(1)	2.113(1)	2.113(1)	2.112(1)	2.113(1)
2.074(1)	2.070(1)	2.071(1)	2.073(1)	2.072(1)	2.073(1)
2.044(1)	2.046(1)	2.046(1)	2.046(1)	2.047(1)	2.045(1)
1.993(1)	1.995(1)	1.993(1)	1.992(1)	1.992(1)	1.992(1)
2.301(1)	2.304(1)	2.303(1)	2.304(1)	2.303(1)	2.302(1)
2.440(1)	2.440(1)	2.439(1)	2.440(1)	2.442(1)	2.444(1)
2.161	2.161	2.161	2.161	2.161	2.161
12.58	12.59	12.58	12.59	12.58	12.59
1.611(1)	1.612(1)	1.612(1)	1.612(1)	1.613(1)	1.611(1)
1.593(1)	1.592(1)	1.589(1)	1.591(1)	1.591(1)	1.591(1)
1.646(1)	1.644(1)	1.645(1)	1.643(1)	1.647(1)	1.646(1)
1.662(1)	1.664(1)	1.663(1)	1.664(1)	1.661(1)	1.663(1)
1.628	1.628	1.627	1.627	1.628	1.628
2.183	2.184	2.181	2.182	2.184	2.183
1.621(1)	1.622(1)	1.622(1)	1.623(1)	1.623(1)	1.621(1)
1.591(1)	1.593(1)	1.593(1)	1.593(1)	1.592(1)	1.591(1)
1.676(1)	1.675(1)	1.676(1)	1.676(1)	1.675(1)	1.677(1)
1.677(1)	1.679(1)	1.679(1)	1.679(1)	1.680(1)	1.675(1)
1.641	1.642	1.642	1.643	1.642	1.641
2.253	2.258	2.258	2.259	2.258	2.253

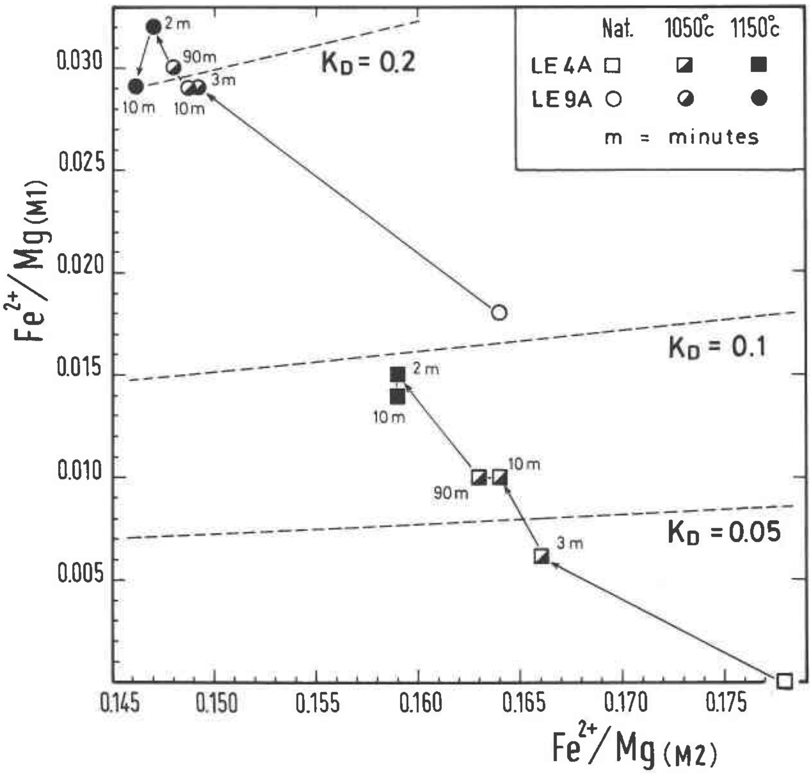

Fig. 1. Relationship between Fe^{2+}/Mg on the M2 site and Fe^{2+}/Mg on the M1 site for natural and heated Le4A and Le9A crystals. Dashed lines: constant distribution coefficients, K_D ($K_D = Fe^{2+}_{M1}Mg_{M2}/Fe^{2+}_{M2}Mg_{M1}$).

electron densities for both M2 and M1, (2) complete site occupancy of T, M2, and M1 sites, (3) charge balance between $^{[4]}Al$ and trivalent ions R^{3+}, and (4) bulk valence balance.

Calculations were performed by means of MINUIT (James and Ross, 1975). Independent variables were all the atomic fractions with completely random initial values in the range 0–1 for M1 and M2 and 0–2 for SiA and SiB sites. Ca^{2+} and Mn^{2+} were assigned to M2 and $^{[6]}Al$, Fe^{3+}, Cr^{3+}, and Ti^{4+} to M1. It will be shown in the following section that the geometrical requirements derived from the structural studies rule out the presence of trivalent ions in the M2 site.

Table 3. Fe^{2+}-Mg site partitioning in natural and heated Le4A and Le9A orthopyroxenes

	Mg_{M1}	Fe_{M1}	Mg_{M2}	Fe_{M2}	K_D
Le4A					
Natural	0.896(3)	0.000(3)	0.818(3)	0.145(3)	0.00
1050 °C, 3 min	0.890(3)	0.006(3)	0.826(3)	0.137(3)	0.04
1050 °C, 10 min	0.888(3)	0.009(3)	0.827(3)	0.136(3)	0.06
1050 °C, 90 min	0.888(4)	0.009(4)	0.828(4)	0.135(4)	0.06
1150 °C, 2 min	0.884(3)	0.013(3)	0.831(3)	0.132(3)	0.09
1150 °C, 10 min	0.885(3)	0.012(3)	0.830(4)	0.132(4)	0.09
Le9A					
Natural	0.965(2)	0.017(2)	0.847(2)	0.139(2)	0.11
1050 °C, 3 min	0.954(3)	0.028(3)	0.859(3)	0.128(3)	0.20
1050 °C, 10 min	0.954(2)	0.028(2)	0.859(2)	0.128(2)	0.20
1050 °C, 90 min	0.953(3)	0.029(3)	0.860(3)	0.127(3)	0.21
1150 °C, 2 min	0.952(3)	0.031(3)	0.861(3)	0.127(3)	0.22
1150 °C, 10 min	0.956(3)	0.028(3)	0.863(3)	0.126(3)	0.20

Note: σ in parentheses.

Heating experiments on the orthopyroxenes

Following X-ray data collection and structural refinement of the natural crystals, the crystal fragments were sealed in quartz tubes in a pure Ar atmosphere (1 atm at room temperature) buffered by iron-wüstite. Runs were carried out sequentially, on the same crystal fragments, for various times, first at 1050 °C and then at 1150 °C (see Table 3). Fragments from Le4A and Le9A were run simultaneously, under identical conditions. Runs were quenched by dropping the charges into cold water and cooled from 1150 to 500 °C in about 0.5 s. It may be that this rate of cooling is too slow to capture equilibrium values at the experimental temperatures (Besancon, 1981; Ganguly, 1982). However, the results reported here show that the experimental procedure that was followed is capable of yielding significant information about the extent of disordering in orthopyroxene at high temperatures.

Following each heating experiment, the two crystals were studied by single-crystal X-ray diffraction methods, and their structures were determined. Mg-Fe^{2+} cation partitioning of natural and heated crystals is summarized in Table 3; standard deviations are deduced from X-ray refinement.

Runs at 950 °C were also carried out on another fragment of Le4, but no evidence of disorder was observed even after 48 h of heating.

RESULTS

Mg-Fe^{2+} disordering

As Virgo and Hafner (1970), Saxena and Ghose (1971), and many other workers have shown by Mössbauer spectroscopy and X-ray diffraction, the heated crystals of orthopyroxene display increased Fe^{2+} in the M1 site. The amount of Fe^{2+} displaced to the M1 site depends on the composition, the temperature to which the crystal was heated, and the length of time for which it was held at this temperature. Crystals Le4A and Le9A have similar Fe^{2+} contents, and at 1150 °C, at least 0.012 Fe^{2+} pfu is displaced into their M1 sites (Table 3).

Increase in disordering of Mg-Fe^{2+} between M1 and M2 is observed after the crystals have been run at temperatures of 1050 °C (Fig. 1) and then quenched.

Because of the high rate of the Mg-Fe^{2+} order-disorder reaction at high temperatures, these heating experiments may not have yielded reliable equilibrium values. Nevertheless there are useful conclusions to be drawn from the data (Table 1; Fig. 1):

1. Before heating of the natural crystals, Le9A was slightly more disordered than Le4A and remained so during the heating experiments.
2. Disordering at high temperatures was observed in Le9A after shorter run times than for Le4A (Fig. 1; Table 3). These differences in behavior presumably reflect the kinetics of reaction. As was inferred from studies of the natural orthopyroxenes (Molin and Varne, in prep.), it may be that the occupation of the M1 site by $^{[6]}$Al inhibits the ready movement of Fe^{2+} from M2 to M1. Recalling that Le4A and Le9A were experimented upon simultaneously, it seems that at 1050 °C, Le4A may have approached equilibrium in about 10 min, whereas Le9A may have approached equilibrium more quickly, before 3 min (Fig. 1). For comparison, Besancon (1981) suggested that his sample HC, with 0.257 Fe^{2+} pfu, may have reached equilibrium in about 11 s at 1000 °C.
3. When the run temperature was increased to 1150 °C, Le4A displayed a significant increase in disorder after quenching, unlike Le9A (Fig. 1). This may be another manifestation of the inhibiting effect of the occupation of M1 by $^{[6]}$Al on Mg-Fe^{2+} ordering during quenching, with disorder more easily quenchable for Le4A than for Le9A, as Saxena et al. (1987) also suggest.

Ordering of $^{[6]}$Al between M1 and M2

Although occupancies of $^{[6]}$Al on M1 and M2 in orthopyroxenes are not obtained from the X-ray refinement, Ganguly and Ghose (1979) were the first to point out that geometrical constraints can be used to infer the extent of $^{[6]}$Al disordering.

Ganguly and Ghose (1979), however, attributed the shortening of the ⟨M2–O⟩ bond length to $^{[6]}$Al disordering, whereas Domeneghetti et al. (1985) showed that the shortening observed by Ganguly and Ghose (1979) was caused by a M2–O3 bond length shortening due to the decreasing occupancy of the SiB site by $^{[4]}$Al. Instead, Domeneghetti et al. (1985) argued that if R^{3+} disordering were to occur in orthopyroxene, it would be revealed by shortening of the four shortest M2–O bond lengths, particularly M2–O1A and M2–O2A. Tazzoli and Domeneghetti (1987) tested this suggestion by heating experiments on aluminous orthopyroxenes from mafic granulites and found no geometrical evidence for disordering of R^{3+} ions. Although the orthopyroxene compositions used in their study are much richer in Fe and Al than the orthopyroxenes of spinel lherzolites, the results reported here support their findings.

The constant mean values among the four shortest M2–O bond lengths in Le4A, and the constant values of the M2–O1A and M2–O2A bond lengths, are incompatible with the presence of appreciable R^{3+} disordering between the M1 and M2 sites (Table 2). In a similar way, although the $^{[4]}$Al content of the SiB tetrahedron may not be directly determinable by structural refinement, the geometrical relationship between the tetrahedral bond lengths and the Si–$^{[4]}$Al substitution is an accurate monitor of the extent of the substitution. It has already been shown (Ganguly and Ghose, 1979; Domeneghetti et al., 1985; Tazzoli and Domeneghetti, 1987) that in orthopyorxenes, $^{[4]}$Al is completely ordered in the SiB site. In these heating experiments on orthopyroxenes from spinel lherzolites, the absence of variations in the length of SiB–O and SiA–O bond lengths (Table 2) may be taken as good evidence against changes in $^{[4]}$Al occupancies with increasing temperature.

SUMMARY AND CONCLUSIONS

Experimental studies of two orthopyroxenes extracted from spinel lherzolite xenoliths showed that Mg-Fe^{2+} disordering that occurred at temperatures of 1050 and 1150 °C may be partially detected after quenching. Disordering occurred more quickly in the orthopyroxene poorer in $^{[6]}$Al, possibly because the occupation of M1 by $^{[6]}$Al inhibits the exchange reaction.

$^{[6]}$Al, Cr^{3+}, and Fe^{3+} are restricted to the M1 site at both low and high temperatures. $^{[4]}$Al remains totally ordered in the SiB site.

ACKNOWLEDGMENTS

The lherzolitic xenoliths were kindly supplied by Dr. A. Cundari. I am grateful to Professor A. Dal Negro, Professor E. M. Piccirillo, and Dr. R. Varne for their comments. Dr. R. Varne revised the manuscript.

Financial support was provided by Ministero della Pubblica Istruzione and C.N.R.: Centro di Studio sui Problemi dello Orogeno delle Alpi Orientali, Padova.

REFERENCES CITED

Besancon, J.R. (1981) Rate of cation disordering in orthopyroxenes. American Mineralogist, 66, 965–973.

Colby, J.W. (1972) MAGIC IV, a computer program for quantitative electron microprobe analysis. Bell Telephone Laboratories, Inc., Allentown, Pennsylvania.

Dal Negro, A., Carbonin, S., Domeneghetti, C., Molin, G.M., Cundari, A., and Piccirillo, E.M. (1984) Crystal chemistry and evolution of the clinopyroxene in a suite of high pressure ultramafic nodules from the Newer Volcanics of Victoria, Australia. Contributions to Mineralogy and Petrology, 86, 221–229.

Della Giusta, A., Princivalle, F., and Carbonin, S. (1986) Crystal chemistry of a suite of natural Cr-bearing spinels with $0.15 < Cr < 1.17$. Neues Jahrbuch für Mineralogie Abhandlungen, 155, 319–330.

Domeneghetti, M.C., Molin, G.M., and Tazzoli, V. (1985) Crystal-chemical implications of the Mg^{2+}-Fe^{2+} distribution in orthopyroxenes. American Mineralogist, 70, 987–995.

Ganguly, J. (1982) Mg-Fe order-disorder in ferromagnesian silicates: Thermodynamics, kinetics, and geological applications. In S.K. Saxena, Ed. Advances in physical geochemistry, p. 58–100. Springer-Verlag, New York.

Ganguly, J., and Ghose, S. (1979) Aluminous orthopyroxene: Order-disorder, thermodynamic properties and petrologic implications. Contributions to Mineralogy and Petrology, 69, 375–385.

International tables for X-ray crystallography. (1974) Vol. 4, 99–101. Kynoch Press, Birmingham, England.

James, F., and Ross, M. (1975) MINUIT, a system for function minimisation and analysis of the parameter errors and correlations. Computer Physics, 10, 343–347, CERN/DD, International Report 75/20.

North, A.C.T., Phillips, D.C., and Mathews, F.S. (1968) A semi-empirical method of absorption correction. Acta Crystallographica, A24, 351–359.

Princivalle, F., and Secco, L. (1985) Crystal structure refinement of 13 olivines in the forsterite-fayalite series from volcanic rocks and ultramafic nodules. Tschermaks Mineralogische und Petrographische Mitteilungen, 34, 105–115.

Rossi, G., Smith, D.C., Ungaretti, L., and Domeneghetti, M.C. (1983) Crystal chemistry and cation ordering in the system diopside-jadeite: A detailed study by crystal structure refinement. Contributions to Mineralogy and Petrology, 83, 247–258.

Saxena, S.K., and Ghose, S. (1971) Mg^{2+}-Fe^{2+} order-disorder and the thermodynamics of the orthopyroxene–crystalline solution. American Mineralogist, 56, 532–559.

Saxena, S.K., Tazzoli, V., and Domeneghetti, M.C. (1987) Kinetics of Fe^{2+}-Mg distribution in aluminous orthopyroxenes. Physics and Chemistry of Minerals, 15, 140–147.

Tazzoli, V., and Domeneghetti, M.C. (1987) Crystal-chemistry of natural and heated aluminous orthopyroxenes. Physics and Chemistry of Minerals, 15, 131–139.

Tokonami, M. (1965) Atomic scattering factor for O^{2-}. Acta Crystallographica, 19, 486.

Virgo, D., and Hafner, S.S. (1970) Fe^{2+}, Mg order-disorder in natural orthopyroxenes. American Mineralogist, 55, 201–223.

Zachariasen, W.H. (1963) The secondary extinction correction. Acta Crystallographica, 16, 1139–1144.

Manuscript received December 7, 1987
Manuscript accepted January 3, 1989